Effect of small-scale architecture on polymer mobility

Jutta Luettmer-Strathmann[a)]
Department of Physics, The University of Akron, Akron, Ohio 44325-4001

(Received 19 November 1999; accepted 20 December 1999)

Processes on different length scales affect the dynamics of chain molecules. In this work, we focus on structures on the scale of a monomer and investigate polyolefins, i.e., hydrocarbon chains with different small-scale architectures. We present an exact enumeration scheme for the simulation of interactions and relative motion of two short chain sections on a lattice and employ it to deduce the probability for segmental motion for polymers of four different architectures in the melt. The probability for segmental motion is inversely proportional to the monomeric friction coefficient and hence the viscosity of a polymer. Combining our simulation results with an equation of state for the thermodynamic properties of the polymers, we are able to make predictions about the variation of the friction coefficient with temperature, pressure, and small-scale architecture. To compare our results with experimental data, we have determined monomeric friction coefficients from experimental viscosity data for the four polyolefins considered in this work. For temperatures well above the glass transition temperature, we find that our simple approach gives a good qualitative representation of the variation of the friction coefficient with chain architecture, temperature, and pressure. © *2000 American Institute of Physics.* [S0021-9606(00)50311-0]

I. INTRODUCTION

The dynamics of chain molecules are affected by local interactions between individual chain segments as well as processes on the length scale of the whole chain and collective motions of chain segments. In this work, we investigate the effect of small-scale chain architecture on the dynamic properties of polymers. The polyolefins depicted in Fig. 1 are a good example for this effect. These polyolefins, all hydrocarbons with sum formula C_nH_{2n}, differ considerably in their viscoelastic properties[1–10] despite their chemical similarity.

An important ingredient in theories for polymer dynamics is a friction coefficient ζ which is employed in coarse-grained models to describe small-scale effects on the dynamics of the system (cf. Ref. 11). In the Rouse model, for example, chain segments consisting of many monomers are represented by a single bead and spring. The Rouse friction coefficient ζ_R describes the damping of the bead motion by the surrounding medium. The Rouse viscosity η_R is proportional to ζ_R and given by[11]

$$\eta_R=\frac{N_A}{36}\rho\frac{R_0^2}{M}N_R\zeta_R, \tag{1}$$

where N_A is Avogadro's number, ρ is the mass density, M is the molecular mass, R_0^2 is the mean-squared end-to-end distance of the chain, and N_R is the number of Rouse segments per chain. The Rouse model describes the viscosity of polymer melts of sufficiently short chains, i.e., for polymers with a molecular mass well below the entanglement mass M_e. For larger molecular masses, entanglement effects have to be taken into account.[11] While ρ and R_0^2 vary with temperature at constant pressure, almost all of the temperature dependence of the viscosity is contained in the friction coefficient.[1] Since the viscosity increases strongly as the glass transition temperature is approached, the friction coefficient ζ reflects collective motion as well as small-scale interactions.

The friction coefficient ζ is inversely proportional to the probability for segmental motion,[12] a relationship that we are going to exploit in this work. In an exact enumeration procedure we perform lattice simulations of relative motion and interactions of two short chain segments, where the surrounding medium is represented in an average way. The collected statistics are evaluated as described in Sec. II to yield the average probability for segmental motion as a function of a reduced temperature and lattice filling fraction for each of the architectures in Fig. 1.

In Sec. III we combine our simulation results with the recently developed Born–Green–Yvon lattice model for the thermodynamic properties of polymers[13–15] to investigate the mobility of the four polyolefins at given temperature and pressure. Our method of determining the friction coefficients is not an absolute one, but using the probability for segmental motion of a linear chain (polyethylene in our case) at 413 K and atmospheric pressure as a reference value we are able to calculate relative values of the friction coefficients as a function of temperature and pressure.

In order to compare our results with experimental data, we extract friction coefficients of the polyolefins of interest from experimental viscosity data as described in Sec. IV. For temperatures well above the glass transition temperature, we find that our approach gives a good qualitative representation of the variation of the friction coefficient with temperature and chain architecture. We also compare the pressure dependence of the viscosity of polypropylene[16] with our predictions and find very good agreement for low to moderate pressures. The results presented here as well as future directions of this work are discussed in Sec. V.

a)Electronic mail: jutta@physics.uakron.edu

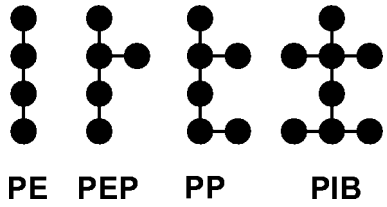

FIG. 1. United atom representation of the polyolefins considered in this work. Shown are the repeat units with four carbon atoms in the backbone for polyethylene (PE), an alternating copolymer of polyethylene and polypropylene (PEP), polypropylene (PP), and polyisobutylene (PIB).

II. SIMULATION OF LOCAL MOBILITY

A central point of this work is the determination of the probability of segmental motion from a consideration of two short chain segments in a dense medium. To this end we perform an exact enumeration of all possible combined configurations and relative movements of two chain segments on a lattice. During the enumeration procedure we collect statistics on the characteristic parameters of each possible initial and final configuration and the connecting move. In a second step, these statistics are evaluated for conditions corresponding to different temperatures and densities. The advantage of this two-step procedure is that the time-consuming part, the exact enumerations, have to be performed only once to yield results that can be evaluated quickly for a variety of conditions.

A. Procedure

For each of two polymer molecules, referred to as chain one and chain two from now on, we consider a straight section composed of three repeat units with given (generally not identical) side group arrangements. The repeat unit in the middle is the section of interest in each case, while the attached units represent the rest of the (long) chains. As depicted in Fig. 1, we employ repeat units with four carbon atoms in the backbone for all the polyolefins considered here. The simulation procedure is illustrated in Fig. 2.

In a preparatory step, all possible conformations (side-group arrangements of the three-repeat-unit sections) of the chains are generated. The basic step in the enumeration, to be described below, is performed for given conformations and relative orientation of the chains. Keeping the conformation and orientation of chain one fixed, the basic step is repeated for all orientations of chain two. This sequence of steps is then repeated for different chain-two conformations until all conformations of chain two are exhausted. Then the whole sequence is repeated for all different chain-one conformations. This assures that we enumerate the results for all possible and distinct combined configurations of the chains.

In a basic step, the section of interest of chain one is fixed to the origin of a simple cubic lattice and aligned with the z axis. The total number n_t and the coordinates of the nonbonded nearest-neighbors (nn) sites are determined as is the maximum number $c_m = 4s_f$ of possible contacts, where s_f denotes the number of lattice sites occupied by the section of interest. For a polyethylene (PE) chain, for example, the section of interest occupies $s_f = 4$ sites, has $n_t = 16$ nearest neighbor sites and a maximum of $c_m = 16$ contacts, while for polyisobutylene (PIB) the values are $s_f = 8$, $n_t = 24$, and $c_m = 32$.

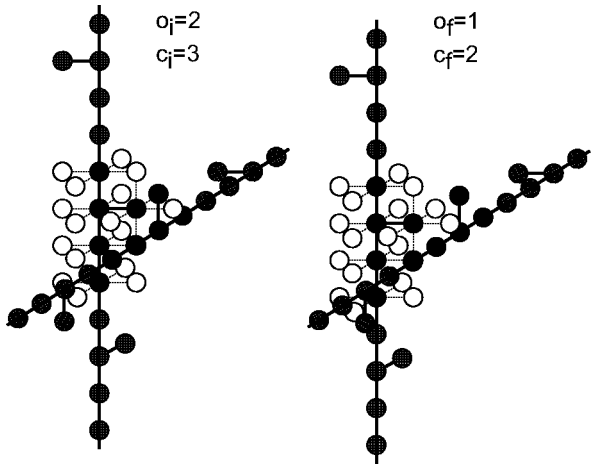

FIG. 2. Illustration of the simulation procedure. The figure on the left shows an initial combined configuration of two PEP segments. There are $s_f = 5$ sites in the section of interest in each chain, indicated by the dark filled circles, and $n_t = 18$ identified nearest neighbor sites of chain one (indicated by open circles). The numbers o_i and c_i indicate the number of nn sites occupied by chain two and the number of established contacts, respectively. The figure on the right shows the new combined configuration after chain one has been moved one lattice site to the front. The numbers o_k and c_k give occupied sites and established contacts, respectively. In the move, $s_n = 5$ sites were newly occupied by the first segment.

Next, an orientation for chain two is chosen, and the following procedure is repeated for each site of interest of chain two and each identified nearest-neighbor site of chain one, where care has to be taken to avoid double counting. For the given orientation of chain two, contact is made between the chains by moving the currently considered site of chain two onto the currently considered nearest-neighbor site of chain one. If the sections do not overlap, the combined configuration is accepted. It is evaluated by counting how many of the n_t nearest-neighbor sites of chain one are occupied by chain two (this number is called o_i) and by counting the number c_i of contacts between chains established in this way. The numbers (o_i, c_i) characterize the static properties of the initial state.

In order to determine the mobility of the segments, an attempt is made to displace chain one by one lattice site in each of the six directions, $\pm x$, $\pm y$, and $\pm z$, in turn. If the attempt leads to overlap between the chains, it is counted as impossible. Otherwise, the number s_n of lattice sites newly occupied by the first section of interest is counted and the new combined configuration is characterized by determining the numbers o_f and c_f of occupied nn sites and established contacts, respectively. The numbers (o_f, c_f) characterize the static properties of the final state, while the set $(i, f, s_n) \equiv (o_i, c_i; o_f, c_f; s_n)$ characterizes the move.

For the results presented here, the exact enumeration procedure described above was performed for PE, PEP, and PP (polypropylene). To avoid excessive computation times for PIB, we generated representative samples of one eighth of the single chain conformations and proceeded with those as described above. The different representative samples for

the PIB conformations give essentially identical results for the properties presented in this work. The result of the simulations are the frequency of occurrence, $n(i,f,s_n)$, of moves of type (i,f,s_n), as well as statistics on the type, (o_k,c_k), and frequency of occurrence, m_k, of the combined configurations.

B. Evaluation

In order to determine the probability P for segmental motion, we consider the probabilities $P(i,f,s_n)$ for the different types of moves and then form the sum

$$P=\sum_{(i,f,s_n)} P(i,f,s_n). \tag{2}$$

The probability $P(i,f,s_n)$ for a move of type (i,f,s_n) is expressed as

$$P(i,f,s_n)=\frac{n(i,f,s_n)P_iP_{\Delta E}P_\phi}{\Sigma_{f,s_n} n(i,f,s_n)}, \tag{3}$$

where P_i is the probability for the initial combined configuration to be of type (o_i,c_i), $P_{\Delta E}$ accounts for the energy difference $\Delta E=E_f-E_i$ between initial and final states, and P_ϕ is the probability that a sufficient number of contiguous sites is available to the moving segment in a lattice filled to a fraction ϕ.

Both P_i and $P_{\Delta E}$ involve the energy of a combined configuration of chain segments in a dense medium. As explained in detail in Refs. 15 and 17, the energy E_k for a combined configuration characterized by (o_k,c_k) is obtained from

$$E_k=\epsilon\left(c_k+\frac{(n_t\xi-o_k)(c_m-c_k)}{n_t-o_k}\right), \tag{4}$$

where ϵ is the interaction energy between two molecular sites ($\epsilon<0$) and where $\xi=2\phi/(3-\phi)$ is the contact density for infinitely long chains at a filling fraction of ϕ. The contributions to the energy E_k in Eq. (4) are due to contacts between chain one and chain two and between chain one and its randomly filled nearest-neighbor sites, respectively. Please note that in the case of unbranched segments (PE), Eq. (4) implies $E_k=\epsilon c_m\xi$ for all k so that there are no energetically preferred configurations for PE. The unbranched segments thus serve as our reference system which allows the isolation of the effects of small scale architecture.

The probability P_i for an initial combined configuration with energy E_i is proportional to the Boltzmann factor

$$P_i=m_ie^{-\beta E_i}\Big/\sum_k m_ke^{-\beta E_k}, \tag{5}$$

where m_i is the multiplicity of the combination (o_i,c_i) and where $\beta=1/k_BT$ with temperature T and Boltzmann's constant k_B. The effect of energetics on the probability of a move is described using the Metropolis form

$$P_{\Delta E}=\begin{cases} e^{-\beta\Delta E} & \text{if } \Delta E>0 \\ 1 & \text{if } \Delta E\leqslant 0, \end{cases} \tag{6}$$

where $\Delta E=E_f-E_i$.

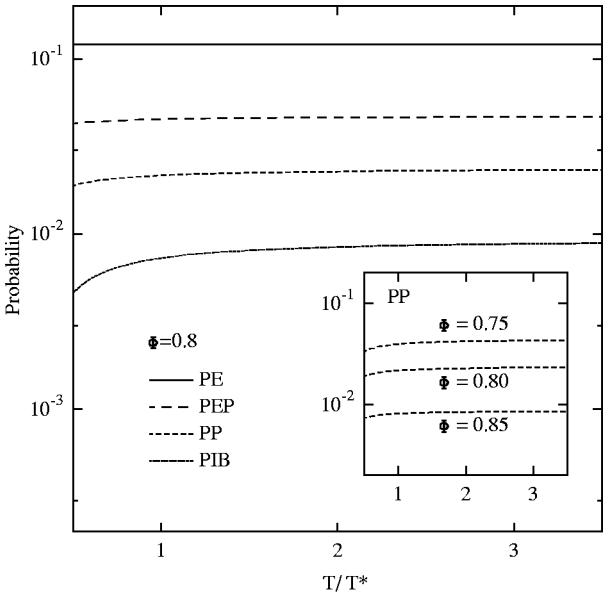

FIG. 3. Probability for segmental motion as a function of reduced temperature $T/T^*=k_BT/\epsilon$ at constant filling fractions ϕ determined from the simulation procedure and Eqs. (2)–(7). The graph shows results for the four different architectures (see Fig. 1) at a common filling fraction of $\phi=0.8$, while the insert displays results for three different filling fractions for the architecture of PP.

The mobility of a chain segment is greatly reduced by the presence of the other chains in its surroundings. Consider, for the moment, monomers on a lattice and the attempt of a single particle to move from one site to a neighboring site. If all of its neighboring sites are occupied, the attempt will certainly fail. But even if a nearest-neighbor site is available, the attempt may fail when another particle is headed for the same site. The only way to guarantee that an attempted move will be successful is to require that a neighboring site as well as its nearest-neighbor sites (except for the one occupied by the particle under consideration) are empty. This is a total of six sites for monomers on a simple cubic lattice. Extending this reasoning to chain molecules, where each monomer is bonded (on average) to two monomers on neighboring sites, we require four empty sites in the neighborhood of each site involved in the move. In terms of our variables introduced above, a volume of $4s_n$ is required in a move in which s_n sites are newly occupied. Assuming a random distribution of voids over the lattice, the probability of finding $4s_n$ lattice sites among the n_t nearest-neighbor sites of the segment of interest is given by[18]

$$P_\phi=\exp\left(-\frac{4s_n}{n_t(1-\phi)}\right), \tag{7}$$

where $(1-\phi)$ is the fraction of empty sites.

In Fig. 3 we present simulation results for the probability of segmental motion, evaluated according to Eq. (2) with Eqs. (3)–(7). The probability P is shown as a function of reduced temperature $T/T^*=k_BT/\epsilon$ for a given filling fraction ϕ for the four architectures considered in this work. The effect of the increasing number of side groups on the mobility is clearly visible. The linear chain (PE) has the highest probability of segmental motion followed by PEP, PP, and

TABLE I. BGY lattice-model parameters for the polyolefins considered in this work (Ref. 15). Please note: The value r for the number of lattice sites per chain is proportional to the molar mass of the polymer. The values presented here correspond to a molar mass of $M=170\,000$ for each of the polyolefins.

Polymer	PE	PEP	aPP	PIB
ϵ(J/mol)	−1977.5	−2000.0	−2040.7	−2208.1
r	14210.6	14226.1	14471.8	13433.8
v(L/mol)	0.013	0.013	0.013	0.013

PIB which have one, two, and four side groups in the four-carbon backbone monomer, respectively. The insert shows the probability P as a function of reduced temperature for three different filling fractions for the PP architecture. As expected, the probability for segmental motion increases with reduced temperature and decreases with filling fraction.

III. CALCULATION OF FRICTION COEFFICIENTS

With a method to obtain the probability for segmental motion in hand, we are now in a position to address the monomeric friction coefficient $\zeta \propto P^{-1}$. The proportionality constant between P^{-1} and ζ is not easily determined. However, as pointed out earlier, our goal is to determine how the local architecture changes the mobility of branched chains compared to that of linear chains. Hence, we choose a reference state for the linear chain and express our results for the friction coefficients as the ratio

$$\frac{\zeta}{\zeta_{\mathrm{ref}}}=\frac{P_{\mathrm{ref}}}{P}, \tag{8}$$

where P_{ref} and ζ_{ref} are the reference state values of the probability of segmental motion and the friction coefficient of the linear chain, respectively. The reference state can be chosen freely; in our case a temperature of $T_{\mathrm{ref}}=413.15$ K and a pressure of $p_{\mathrm{ref}}=0.1$ MPa turn out to be convenient. In order to make contact with experimental data we employ equations of state based on the recently developed Born–Green–Yvon (BGY) lattice model.[13,14] The BGY lattice model has three system-dependent parameters for a polymer melt, corresponding to the volume v per lattice site, the number r of sites occupied by each chain, and the interaction energy ϵ between nonbonded nearest neighbors. For each of the polymers considered in this work, values for the system-dependent parameters have been determined from a comparison with experimental temperature-density-pressure data[15] and are summarized in Table I.

In Fig. 4 we present calculated values for the relative friction coefficient $\zeta/\zeta_{\mathrm{ref}}$ as a function of temperature at a pressure of 0.1 MPa for the polyolefins considered in this work. Please note that the temperature variation here is much larger than that in Fig. 3. While Fig. 3 depicts the probability $P\propto\zeta^{-1}$ at constant ϕ, i.e., at constant density $\rho=\phi/rv$, Fig. 4 shows constant pressure results. It is the temperature variation of the density at constant pressure that, through Eq. (7), is responsible for the strong temperature dependence of $\zeta/\zeta_{\mathrm{ref}}$.

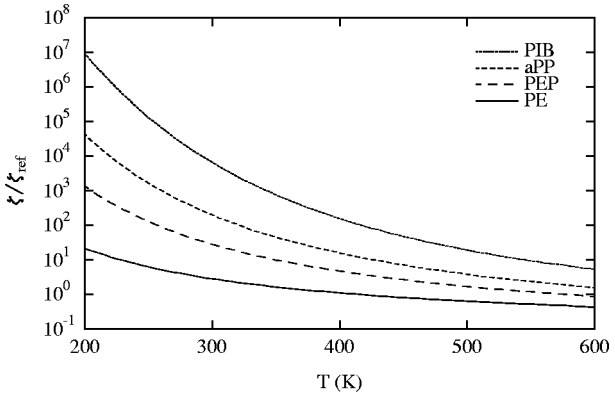

FIG. 4. Calculated friction coefficients $\zeta/\zeta_{\mathrm{ref}}$, as a function of temperature at constant pressure $p=0.1$ MPa for the polyolefins considered in this work. The reference value is obtained for the linear chain (PE) at 413.15 K and 0.1 MPa.

IV. COMPARISON WITH EXPERIMENTAL DATA

The friction coefficient ζ is not a directly measured quantity but can be extracted from measurements of dynamic properties like the viscosity or the self-diffusion coefficient. The most direct access to ζ is through the Rouse viscosity η_{R} described in the Introduction. With the aid of Eq. (1) a friction coefficient per monomer can be defined as follows:

$$\zeta=\frac{N_{\mathrm{R}}\zeta_{\mathrm{R}}}{N}=m_0\frac{\eta_{\mathrm{R}}}{M}\left(\frac{N_A}{36}\rho\frac{R_0^2}{M}\right)^{-1}, \tag{9}$$

where N is the degree of polymerization and m_0 is the mass of a monomer which we take to be $n\times 14.03$ g/mol, where n is the number of carbon atoms in the repeat unit depicted in Fig. 1. In addition to the Rouse viscosities η_{R}/M, evaluation of Eq. (9) requires values for R_0^2, the mean-squared end-to-end distance of the chains, and for ρ, the mass density of the melt. In this work, we employ experimental values for these properties at a temperature of 413 K presented in a recent review by Fetters *et al.*[2] and included in Table II.

The Rouse model describes directly the viscosity for melts of low molecular mass $M\ll M_{\mathrm{e}}$ (for example, $M_{\mathrm{e}}\approx 1000$ for PE and $M_{\mathrm{e}}\approx 7300$ for PIB[2]). Unfortunately, mea-

TABLE II. Experimental parameters for the polyolefins considered in this work. The values correspond to atmospheric pressure and a temperature of 413.15 K. The glass transition temperature for polyethylene (PE) is an estimate based on results for ethylene-butene copolymers (Ref. 21).

Polymer	PE	PEP	aPP	PIB
R_0^2/M (Å^2 mol/g) (Ref. 2)	1.21	0.834	0.67	0.57
ρ (g/cm^3) (Ref. 2)	0.785	0.79	0.791	0.849
M_{e} (Ref. 2)	976	2284	4623	7288
viscosity data references	4,5	6	7	8
temperature range T(K)	350–500	248–443	298–463	298–473
$\log\left(\frac{\eta_{\mathrm{R}}}{M}\Big/\frac{\mathrm{Poise}}{\mathrm{g/mol}}\right)$	−4.1035	−3.6039	−3.3424	−2.7669
log(ζ/Poise cm)	−8.5554	−7.8001	−7.3648	−6.6388
C_1	2.018	3.565	3.101	4.684
C_2 (K)	253	277	189	307
T_{g} (K)	188	211	268	202
T_{g} references	21	6	7	1,3

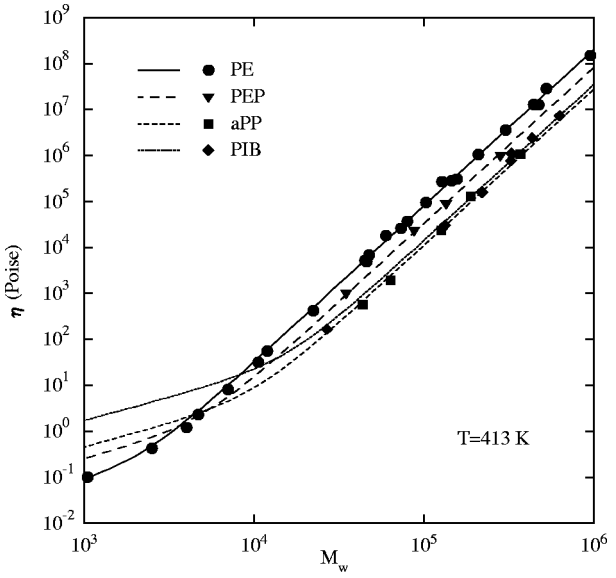

FIG. 5. Viscosity of polyolefin melts as a function of molecular mass M_w. The symbols represent experimental data adjusted to 413 K as explained in the text. The references for the data are Refs. 5, 9, and 10 for PE, Ref. 6 for PEP, Ref. 7 for aPP, and Ref. 8 for PIB. The lines represent the empirical scaling law Eq. (10), where $M_c=2.2M_e$ with M_e from Ref. 2, and where the values for η_R/M have been determined from a comparison with the experimental data. Values for these system-dependent parameters are included in Table II.

surements of the melt viscosities for short chains are not only scarce, but chain-end effects may have to be taken into account in their evaluation.[4] We, therefore, decided to turn to high molecular-weight viscosity data and an empirical scaling relation[19] to extract values for η_R/M. Motivated by the reptation model[11] and by experience with experimental data, Graessley and Edwards[19] suggested the following molecular mass dependence of viscosities in polymer melts:

$$\eta=\frac{\eta_R}{M}\ M\left[1+\left(\frac{M}{M_c}\right)^{2.4}\right], \tag{10}$$

with $M_c=2.2M_e$.[19,20] In principle, Eq. (10) could be compared to experimental viscosity data at a given temperature to extract both η_R and M_c. This, however, is not advisable since the results for η_R and M_c will then strongly depend on the range of molecular weights for which viscosity data are available. Instead, we fix $M_c=2.2M_e$, taking the experimental M_e values at 413 K of Fetters *et al.*[2] quoted in Table II, and fit for η_R/M only. This procedure requires values for the viscosity at 413 K, which we obtain by employing the temperature correlations provided with the experimental data[5–8] to shift the viscosity values from the temperature of the measurements to 413 K. More information on the temperature correlations is provided below. In Fig. 5 we present the data (symbols) for the viscosity at 413 K obtained in this way as a function of molecular mass for the polyolefins considered in this work. The resulting correlations for the mass dependence of the viscosity are represented by the lines in Fig. 5 and are seen to give a satisfactory representation of the experimental data. The values for η_R/M obtained in this way are included in Table II. Inserting them into Eq. (9) and employing the values for m_0, R_0^2, and ρ as discussed, we arrive at the values for the monomeric friction coefficient ζ at 413 K and atmospheric pressure presented in Table II. The value of the friction coefficient for PE at 413 K and 0.1 MPa is the reference value for the experimental friction coefficients, and all further results will be presented as $\zeta/\zeta_{PE}(413\ \mathrm{K})$.

In measurements of viscoelastic properties of polymers, it is customary to describe the temperature dependence of the viscosity by equations of the type[1] Vogel–Tammann–Fulcher (VTF)

$$\ln(\eta(T))=\ln(A)+\frac{1}{\alpha(T-T_0)}, \tag{11}$$

or Williams–Landel–Ferry (WLF)

$$\log(\eta(T))=\log(\eta(T_s))-\frac{C_1(T-T_s)}{C_2+T-T_s}. \tag{12}$$

These equations are equivalent with constants related by $C_2=T_s-T_0$, $C_1C_2\ln(10)=1/\alpha$, and $\ln(A)=\ln(\eta(T_s))-C_1\ln(10)$. Here T_s is an arbitrary reference temperature while T_0 indicates the temperature where the system is no longer able to relax to an equilibrium state in a finite amount of time. Since the dominant contribution to the temperature variation of the viscosity is due to the friction coefficient, it is a reasonable approximation to assign the temperature dependence of the viscosity to the friction coefficient.[1] Some of the experimental works quoted here provide slightly different temperature correlations for the viscosity of samples of different molar masses. When shifting the experimental viscosity data to the reference temperature of 413 K, we employed the correlations appropriate for the molar mass under consideration. For the following comparison with our work, on the other hand, we choose a representative correlation for each polyolefin and bring it into WLF form with a reference temperature of $T_{ref}=413$ K. The corresponding parameters C_1 and C_2 are included in Table II.

The temperature dependent friction coefficients are now obtained from

$$\log(\zeta(T))=\log(\zeta(T_{ref}))-\frac{C_1(T-T_{ref})}{C_2+T-T_{ref}}, \tag{13}$$

with the $\zeta(T_{ref})$ values presented in Table II. In Fig. 6 we present the friction coefficients $\zeta(T)$ divided by the reference value $\zeta_{PE}(413\ K)$ for the polyolefins considered in this work. The heavy lines in the graph indicate the temperature range in which experiments were performed and where the temperature correlations are expected to be most reliable. For each of the polyolefins, a strong increase in the friction coefficient is evident as the temperature is lowered. This increase is due to the slowing of the dynamics of the polymers as the glass transition is approached. The glass transition temperature T_g of polypropylene (aPP) is much higher (cf. Table II) than that of the other three polyolefins considered here. This is apparent in Fig. 6, where the friction coefficients of PE, PEP, and PIB have very similar temperature dependencies, while the aPP friction coefficient curve starts turning up at a much higher temperature and crosses the curve of the friction coefficient for PIB.

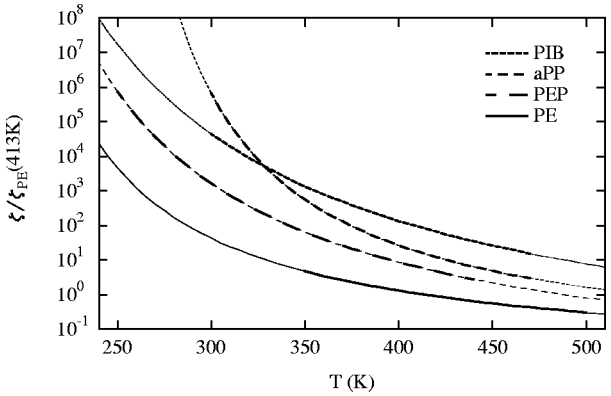

FIG. 6. Temperature dependence of the friction coefficients $\zeta(T)/\zeta_{PE}(413\ \mathrm{K})$ extracted from experimental data. The heavy lines in the graph indicate the temperature range over which experiments were performed. cf. Table II.

In Fig. 7 we present the friction coefficients extracted from experimental viscosity data together with those predicted from our simulation procedure for temperatures well above the glass transition temperatures of the polymers. Comparing the predicted with the ''experimental'' curves we note that in both graphs the values of the friction coefficients increase for a given temperature when going from PE, which has the lowest friction coefficient, over PEP, PP, to PIB. As noted earlier, this can be understood as a result of the different small scale architectures since the number of side groups

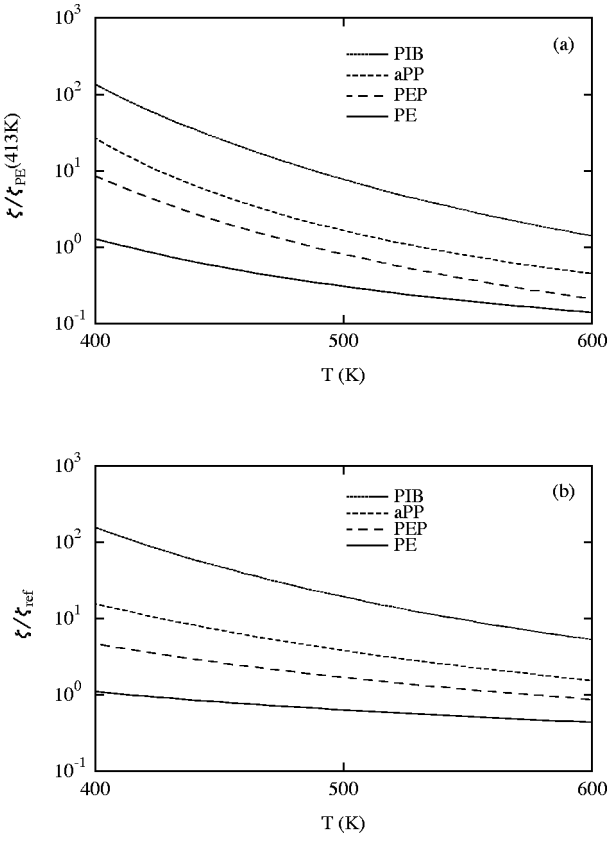

FIG. 7. Friction coefficients extracted from experimental data (a) and predicted from our simulation procedure (b) as a function of temperature at atmospheric pressure.

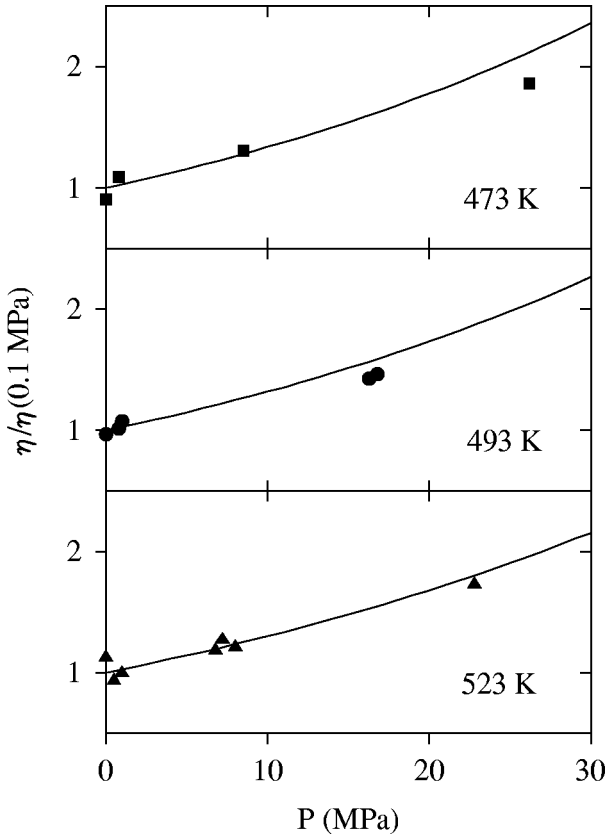

FIG. 8. Pressure dependence of the viscosity of polypropylene. For each of the three isotherms we present viscosities divided by their value at atmospheric pressure. The lines represent results from our simulation procedure, the symbols indicate experimental data by Mattischek and Sobczak (Ref. 16).

in the repeat unit increases from PE (0) over PEP (1), PP (2) to PIB (4). The magnitude of the architecture effect is similar in the predicted and experimental friction coefficients. Furthermore, we note that the variation of the friction coefficients with temperature is of the same order of magnitude in the predicted and extracted curves. While the temperature range in Fig. 7 is well above the glass transition temperatures, lower temperatures are included in Figs. 4 and 6. As can be seen from these figures, the agreement between the simulation results and the ζ values extracted from experimental data diminishes as the glass transition temperature is approached. This is because our simple approach focuses on individual segmental motion rather than cooperative effects, a point which will be discussed below.

In Fig. 8 we compare the pressure dependence of the viscosity of polypropylene as predicted from our work with experimental data[16] along three isotherms. To separate temperature and pressure effects, we use the values of the viscosity at atmospheric pressure to scale the viscosities on each isotherm. For low to moderate pressures ($\leqslant$20 MPa) the agreement is excellent. As the pressure increases further, our work overestimates the viscosity. This is likely due to our employing the BGY-lattice-model equation of state with parameters optimized for low pressures,[15] an issue which will be addressed in future work.

V. DISCUSSION

In this work, we presented an exact enumeration method for lattice simulations of chain segment mobility. The algorithm enumerates the attempted and successful moves for two short, straight sections of a polymer and is evaluated by taking relative frequency, energetics, and density effects into account. The result is the mean probability for segmental motion as a function of reduced temperature and the filling fraction of the lattice. We performed simulations for four different small-scale architectures obtaining results that show a sensible decrease in mobility with increasing density and number of side groups of a monomer.

Combining these results with equations of state for the corresponding polyolefins, we deduce monomeric friction coefficients as a function of temperature and pressure. Our method is not an absolute one, but employing the friction coefficient of polyethylene at 413 K and atmospheric pressure as a reference value, we can predict the relative values of the friction coefficients as a function of temperature and pressure for the polyolefins considered in this work. If we are interested in the properties of a single polyolefin, we can employ the value of the viscosity for a particular temperature and pressure as a reference value and predict the relative variation of the viscosity with temperature and pressure from there. The same is true for other transport properties that depend in a simple way on the friction coefficient; this will allow us to investigate diffusion coefficients, for example, in future work.

To compare our results with experimental data, we extracted Rouse viscosities and monomeric friction coefficients from high molecular mass viscosity data. Employing temperature correlations of the experimental data in the WLF form we obtain experimental monomeric friction coefficients at atmosperic pressure over a range of temperatures, which we scale by the value for PE at 413 K. The comparison of these extracted friction coefficients with the results from our new simulation method is encouraging: For temperatures well above the glass transition temperature the calculated probabilities give a good qualitative representation of the relative variation of the friction coefficient with temperature and monomer architecture. A comparison of calculated and experimental pressure variation of the viscosity of polypropylene along three isochores shows excellent results for lower pressures.

In order to extend the range of validity of the present theory to temperatures closer to the glass transition, cooperative effects in the dynamics will have to be taken into account in a more sophisticated way. In this first work with the new simulation method, we have assumed a random distribution of voids over the lattice and take the system to be in an equilibrium state before each attempted move. One way to improve on this approximation would be to employ an iterative approach in which the distribution of configurations after a round of attempted moves is used as the input distribution of configurations for the next round of moves. Finally, the simulation method introduced here was applied only to straight chain sections of polymers on a cubic lattice with a single site–site interaction strength ϵ. It is, however, readily modified to include chain flexibility, chemical differences and realistic bond angles, which allows a large range of polymeric systems to be investigated in this way. We plan to extend the theory in these directions and are currently focusing on the effects of chain flexibility.

ACKNOWLEDGMENT

Financial support through a faculty research grant from the University of Akron is gratefully acknowledged.

[1] G. C. Berry and T. G. Fox, Adv. Polym. Sci. **5**, 261 (1968).
[2] L. J. Fetters, D. J. Lohse, D. Richter, T. A. Witten, and A. Zirkel, Macromolecules **27**, 4639 (1994).
[3] K. L. Ngai and D. J. Plazek, in *Physical Properties of Polymers Handbook*, edited by J. E. Mark (AIP, Woodbury, NY, 1996), Chap. 25, pp. 341–363.
[4] D. S. Pearson, G. Ver Strate, E. von Meerwall, and F. C. Schilling, Macromolecules **20**, 1133 (1987).
[5] D. S. Pearson, L. J. Fetters, W. W. Graessley, G. Ver Strate, and E. von Meerwall, Macromolecules **27**, 711 (1994).
[6] C. B. Gell, W. W. Graessley, and L. J. Fetters, J. Polym. Sci., Part B: Polym. Phys. **35**, 1933 (1997).
[7] D. S. Pearson, L. J. Fetters, L. B. Younghouse, and J. W. Mays, Macromolecules **21**, 478 (1988).
[8] L. J. Fetters, W. W. Graessley, and A. D. Kiss, Macromolecules **24**, 3136 (1991).
[9] C. R. Bartels, B. Crist, and W. W. Graessley, Macromolecules **17**, 2702 (1984).
[10] J. von Seggern, S. Klotz, and H.-J. Cantow, Macromolecules **24**, 3300 (1991).
[11] M. Doi and S. F. Edwards, *The Theory of Polymer Dynamics* (Clarendon, Oxford, 1986).
[12] F. Bueche, J. Chem. Phys. **20**, 1959 (1952).
[13] J. E. G. Lipson, Macromol. Theory Simul. **7**, 263 (1998).
[14] J. E. G. Lipson and S. S. Andrews, J. Chem. Phys. **96**, 1426 (1992).
[15] J. Luettmer-Strathmann and J. E. G. Lipson, Macromolecules **32**, 1093 (1999).
[16] J.-P. Mattischek and R. Sobczak, Rev. Sci. Instrum. **68**, 2101 (1997).
[17] J. Luettmer-Strathmann and J. E. G. Lipson, Phys. Rev. E **59**, 2039 (1999).
[18] M. H. Cohen and D. Turnbull, J. Chem. Phys. **31**, 1164 (1959).
[19] W. W. Graessley and S. F. Edwards, Polymer **22**, 1329 (1981).
[20] N. P. T. O'Connor and R. C. Ball, Macromolecules **25**, 5677 (1992).
[21] J. M. Carella, W. W. Graessley, and L. J. Fetters, Macromolecules **17**, 2775 (1984).